Dandao Xuebao/Journal of Ballistics
ISSN: 1004-499X
Vol. 35 No. 3 (2023)

Optimizing Resistance Spot Welding for Enhanced Strength and Nugget Formation: A Taguchi Approach.

Sachin K. Dahake[1], Nilesh Diwakar[2], Shyamkumar D. Kalpande[3]
[1]Research Scholar, Department of Mechanical Engineering, RKDFIST SRK University, Bhopal, India.
sachindahake@gmail.com
[2]Professor, Department of Mechanical Engineering, RKDFIST SRK University, Bhopal, India.
[3]Professor, Department of Mechanical Engineering, GCOERC, Nashik, India.

Abstract:- This manuscript provides a comprehensive analysis of resistance spot welding (RSW), including its technique, empirical research, and findings. The text outlines a comprehensive methodology known as Design of Experiments (DOE) that integrates optimization techniques to study the weld strength and nugget formation of AISI 316L steel grade sheets. The study utilizes many methods including tensile shear testing, destructive weld testing with acid etching, and microstructure analysis using specialized equipment like as the inverted microscope. This study utilized the Taguchi technique and signal-to-noise (S/N) ratio analysis to assess how welding current, pressure and weld time affect the tensile strength and nugget of spot welds. The study's findings demonstrate the optimal setups based on empirical experiments, emphasizing the significant impact of welding current on weld strength. This study thoroughly examines the impact of welding conditions on nugget diameter, tensile-shear strength, and microstructure characteristics such as the fusion zone and heat-affected zone. Studying the microstructure offers valuable insights into how welding factors affect weld properties, including recommendations for ideal welding conditions.

Keywords: SS 316L, Nugget diameter, Microstructure, Taguchi Technique

1. Introduction

Resistance spot welding (RSW) is a crucial method for connecting metallic materials because of its high efficiency and cost-effectiveness in diverse industries such as automotive, aerospace, and manufacturing [01-04]. AISI 316L, a frequently utilized stainless steel type, is commonly employed in crucial applications that require exceptional corrosion resistance and mechanical strength [2, 5 & 6]. The mechanical properties of resistance spot welding (RSW) joints in AISI 316L steel are influenced by many process parameters, such as welding current, time, pressure, and electrode shape [06-08]. Although RSW is widely used, there is still a major need for comprehensive studies to fully understand how these parameters impact the mechanical properties of AISI 316L joints [09-11]. Past research has investigated the impact of process parameters on the mechanical characteristics of welded joints in various materials [12-14]. Nevertheless, a comprehensive examination targeting AISI 316L steel joints is necessary [15]. Optimizing the process parameters for resistance spot welding (RSW) of AISI 316L joints is essential to attain the desired mechanical qualities, such as tensile strength, hardness, and fatigue behaviour [16-18]. Furthermore, it is important to have a more profound comprehension of the microstructural alterations caused by different welding conditions to improve the mechanical effectiveness of these connections [19- 21]. Furthermore, given the wide range of uses for AISI 316L, including in settings that are prone to corrosion such as maritime and chemical processing, it is crucial to thoroughly investigate the impact of welding conditions on its resistance to corrosion [2, 22, 23]. An examination of the relationship between process parameters and the microstructure, mechanical characteristics, and corrosion resistance of RSW joints in AISI 316L steel will make a substantial contribution to enhancing the welding process for various industrial uses [24-26].

Therefore, this work seeks to fill the current void in the research by undertaking a thorough examination of how process parameters affect the mechanical properties, microstructure, and corrosion resistance of RSW joints in AISI 316L steel. By conducting thorough testing and analysis, the goal is to optimize the welding conditions to create strong and long-lasting joints. This aims to address the current requirement for a more profound comprehension of this essential feature in welding technology. The influence of welding current and electrode force on the creation of microstructure in the nugget zone and the resulting failure patterns in resistance spot

welded (RSW) joints are important factors that affect the overall mechanical characteristics and performance of the joints. The welding current directly impacts the heat generated during the resistance spot welding (RSW) process [05]. Elevated welding currents result in augmented heat input, which impacts the development of the weld nugget. Elevated temperatures can lead to an increase in grain size and coarsening in the nugget area [14, 15]. Variations in welding current have an impact on the grain size and morphology within the nugget zone. Elevated currents might lead to the formation of bigger grains as a result of heightened thermal energy, which can potentially impact mechanical qualities like as hardness and tensile strength [06, 27]. Use of excessive welding current can result in the development of large grains and unwanted phases, causing brittleness and vulnerability to cracking in the nugget or heat-affected zone (HAZ) [06, 28]. This can lead to premature failure when subjected to mechanical or thermal stress. Liquid metal embrittlement (LME) is a phenomenon where elevated welding currents can induce embrittlement and eventual failure, especially in dissimilar material joints. This occurs when the liquid phase generated at higher temperatures diffuses into the base material, causing embrittlement [14, 29]. The size and shape of the nugget are affected by the force applied to the electrode, which in turn determines the contact area and pressure on the materials being welded [30]. Increased forces often result in bigger nugget sizes as they promote more material deformation and higher heat concentration at the joint contact [07, 31].

Hence, the appropriate application of electrode force guarantees an equal distribution of pressure along the joint contact, resulting in a more uniform microstructure within the nugget zone [01, 32]. Insufficient electrode force can cause incomplete fusion or inadequate penetration at the interface, resulting in weak or intermittent bonding and eventual joint failure [09, 33]. Inadequate electrode force can result in insufficient nugget production or weak bonding between the sheets, leading to failure through either nugget pullout or shear mechanisms when subjected to a load [10, 34]. The ideal welding current and electrode force are crucial for obtaining favorable microstructures and reducing the occurrence of failures in resistance spot welding joints. It is essential to maintain a balance between these factors to achieve the appropriate amount of heat input for the creation of a good nugget, while also avoiding negative consequences such as the enlargement of grain size, fragility, or inadequate bonding. It is crucial to have a methodical comprehension and management of these aspects to create strong and dependable resistance spot welding (RSW) connections in AISI 316L steel, hence improving their mechanical characteristics and overall effectiveness.

2. Material and method

Grade 316L is a type of steel that contains molybdenum, which enhances its resistance to corrosion. Compared to grade 304, grade 316L has superior overall corrosion resistance, especially in chloride conditions, making it more resistant to pitting and crevice corrosion [35]. The study focused on investigating the properties of AISI 316L grade steel sheets. Stainless steels are alloys made primarily of iron and containing a minimum of 10.5% Chromium. Their stainless qualities are attained by the development of a transparent and adhesive coating rich in chromium oxide. Alloy 316L is a versatile austenitic stainless steel characterized by a face-centered cubic structure. AISI 316L stainless steel is a type of stainless steel that is specifically designed for the first shaping into wrought items. The material in question is designated as 316L according to AISI standards. In its annealed state, it is essentially devoid of magnetic properties and can only be made harder through the process of cold working. The reduced carbon concentration, in comparison to alloy 302, provides enhanced corrosion resistance in welded constructions. Austenitic Cr-Ni 316 Stainless steel exhibits superior corrosion resistance qualities compared to type 302. 316L possesses high ductility and exhibits exceptional characteristics in terms of drawing, forming, and spinning. Due to its low carbon content, there is a reduced occurrence of carbide precipitation in the heat-affected zone during welding, resulting in a decreased vulnerability to intergranular corrosion. The chemical composition of AISI 316L, utilized for the current experiments, is presented in Table 1. The composition was determined using spectromaxx, as depicted in Figure 1.

Table 1: Chemical Composition of 316L Stainless Steel

Grade	C%	Mn%	P%	S%	Si%	Cr%	Ni%	Mo%
316L	0.022	1.25	0.045	0.004	0.42	16.16	10.03	2.06

Fig. 1 Spectromaxx (To check the chemical composition of 5-based alloy metals i.e. Fe, Cu, Al, Zn & Ni.)

Types 316 and 316L are austenitic stainless steels that contain molybdenum. They offer greater resistance to general corrosion and pitting/crevice corrosion compared to ordinary chromium-nickel austenitic stainless steel, like type 304. Additionally, these alloys have superior resistance to deformation under constant load, increased resistance to fracture under stress, and enhanced ability to withstand stretching forces at high temperatures. Types 316 and 316L often have a molybdenum content of 2 to 3% to enhance their corrosion resistance. Furthermore, it possesses exceptional corrosion resistance and exhibits high levels of strength. Both types 316 and 316L alloys exhibit exceptional fabricability and formability, characteristic of austenitic stainless steels. Stainless steel 316L exhibits superior properties in terms of creep resistance, stress rupture resistance, and tensile strength at high temperatures when compared to chromium-nickel austenite stainless steel.

2.1 Taguchi method for experimentation

The analysis utilized the Taguchi technique, a resilient design of experiments strategy, to examine the impact of machine parameters on the tensile strength of AISI 316L welded joints.

Variables: Welding current (KA), Pressure (Bar), Weld time (Cycles).

Levels: Each factor was evaluated at three specific levels: 6, 8, and 10 for welding current; 2, 4, and 6 for pressure; and 4, 6, and 8 for weld duration. Performed welding trials on AISI 316L steel samples utilizing various parameter combinations using the Taguchi L9 orthogonal array. Measurements of tensile strength (in kilograms-force) were recorded for each welded junction.

2.2 Signal-to-Noise ratio (S/N ratio)

Utilized Taguchi analysis to determine the Signal-to-Noise Ratio (S/N Ratio) for every combination of welding parameters (A1). Calculated the average of the measured tensile strength values (MEAN1) for each parameter setting.

2.3 Data collection and analysis

Compiled and organized the recorded tensile strength readings acquired from the welding trials for every possible combination of welding settings. Examined the Signal-to-Noise Ratio (A1) and MEAN1 to determine the most effective parameter configurations for maximizing the tensile strength in AISI 316L welded joints. The study employed the Taguchi technique to investigate the impact of welding current, pressure, and weld duration on the tensile strength of AISI 316L welded joints. The inquiry sought to identify the ideal parameter combinations that would maximize the tensile strength of the welded joints for this particular material composition, using a methodical experimental design and analysis.

The Taguchi method consists of the following steps:

1. Identify the primary function that has to be optimized, together with its associated side effects and potential failure mode.
2. Identification of noise factors, testing settings, and quality criteria is required.
3. Determination of the primary function to be optimized.
4. Identify the control variables and their corresponding levels.
5. Choosing an orthogonal array and matrix experiment.
6. Performing the matrix experiment.
7. Analyzing the data and predicting the optimal level.
8. Assessing the impact of the parameters on the performance.
9. Conducting the verification experiment and strategizing the next actions.

2.4 Preparation of the specimen

A 0.4 mm thick metal sheet made of SS 316L is divided into 9 pieces using an EDM machine. Each piece has dimensions of 100 mm x 25 mm. The base metal was cut into plates measuring 100 x 25 mm (length x width) and joined together using a lap joint measuring 15 x 15 mm, following the AWS C1.1M/C1.1:2012 standard, as depicted in figure 2.

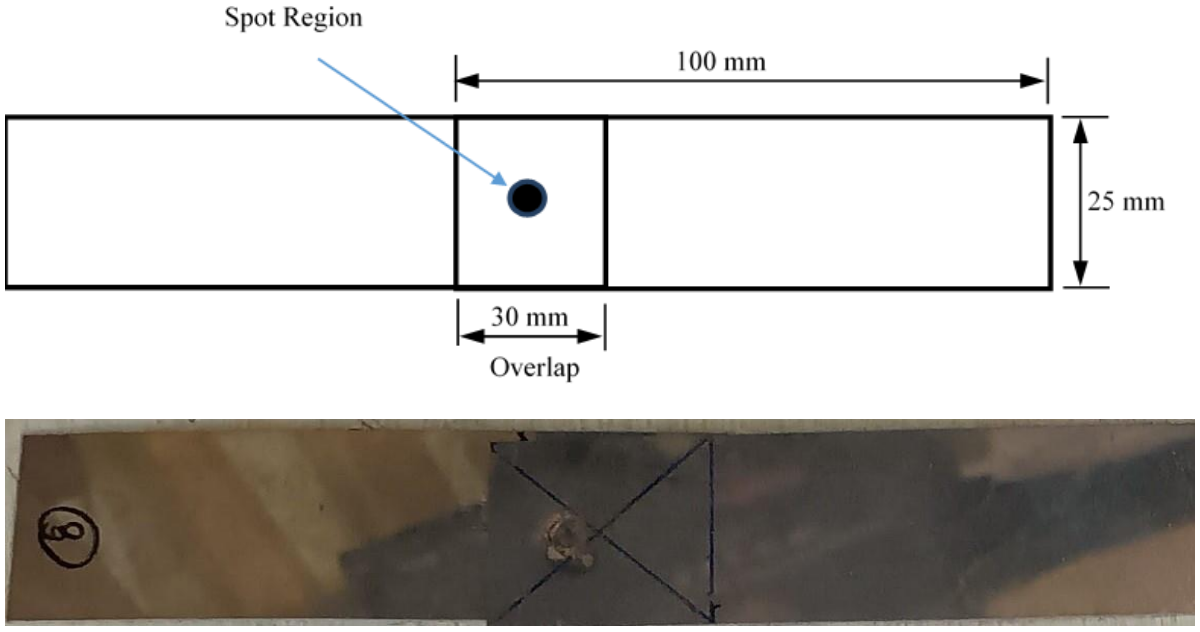

Fig. 2 Sample Specimen

3. Implementation of methodology

To achieve the required objectives, the approach of Design of Experiments (DOE) combined with optimization techniques is selected. A thorough examination of existing literature is conducted, and a process for conducting the experiments is established. The workflow for analyzing the data is then explained as follows:

1. Strategic formulation
   a) Determining the location for the experiment
   b) Determination of optimal values for input parameters (electrode force, welding current, weld time).
   c) Material Selection.
   d) The choice of an orthogonal array, specifically the L9 Orthogonal Array.
2. Conducting the Experiment Measuring the Responses (Tensile Strength)

3. Utilization of Minitab software for analysis.
   a) Calculate the Signal to Noise (S/N) ratio.

$$\left(S/N\right) = -10\log\left(1/n\sum_{i}^{n} y_i^2\right)$$

   b) Creation of the Inner Array utilizing the provided input parameters
   c) Creation of an Outer Array utilizing Responses
   d) Application of Taguchi Analysis in Experimental Design
   e) Analyzing the Taguchi results to determine the optimal settings for electrode force, welding current, and weld duration. Regarding the specified objective function
4. Implementation of a program to determine the most favorable values

An experimental study utilized an electrical resistance spot-welding equipment that was regulated by both current and time. The capacity of the device is 120 kVA and it utilizes a pneumatic application mechanism. The parts were joined together using electrical resistance spot welding, with adjustments made to the electrode force, welding current, cycle time, and the diameter of the fixing electrode, which had a sphere of 15 mm. The cooling water flow rate was also varied during the experiments. The experimental setup is shown in the figure 3 and control panel of the machine is in figure 4.

- The welding current options are 6, 8, and 10 KA [09].
- Electrode Force: 2, 4, and 6 bars.
- The duration of the welding process is 4, 6, and 8 cycles [10, 11].
- The duration of Squeeze Time is consistently 35 seconds.

Fig. 3 Experimental setup

Fig. 4 Digital display of control panel

3.1 Design of experiment (DoE) and testing results

DoE is a systematic approach to the investigation of a system or process. A series of structured tests are designed in which planned changes are made to the input variables of a process or system. The effects of these changes on a pre-defined output are then assessed. For each input variable, several levels are defined that represent the range

for which the effect of that variable is desired to be known. An experimental plan is produced which tells the experimenter where to set each test parameter for each run of the test. The response is then measured for each run. The method of analysis is to look for differences between response (output) readings for different groups of input changes. The ideal course of action is to construct an experiment so that accurate, reliable, and good findings can be drawn swiftly, effectively, and economically whenever multiple factors affect a product characteristic. During a DOE experiment, input factors are manipulated to see how they affect the output variables of a system or process. The concept of DOE can be used in both real-world systems and digital simulations. The purpose of good experimental design is to maximise the quantity of knowledge obtained through an investigation while minimising the amount of data needed for that study. In factorial experiments, rather than adjusting just one variable at a time, multiple variables are altered in combination to determine their combined impact. The level of sensitivity to each element and the combined effect of two or more factors can be estimated using a factorial design. Table 2 is indicating the levels of welding current (KA), Pressure (Bar) and Weld time (Cycle) taken in the DoE.

Table 2: Design of Experiment with testing results

Welding current (KA) – (A)	Pressure (Bar) – (B)	Weld time (Cycles) – ©	Tensile strength (Kgf)	SNRA1	MEAN1
6	2	4	272.12	48.6952	272.12
6	4	6	199.21	45.9862	199.21
6	6	8	131.82	42.3996	131.82
8	2	6	231.05	47.2741	231.05
8	4	8	269.40	48.6080	269.40
8	6	4	248.90	47.9205	248.90
10	2	8	254.20	48.1035	254.20
10	4	4	271.64	48.6799	271.64
10	6	6	285.12	49.1006	285.12

Figure 5 are the specimens prepared after Spot Weld of above combination and marked with numbers. These specimens are prepared in the in one of the welding Industry at Nashik.

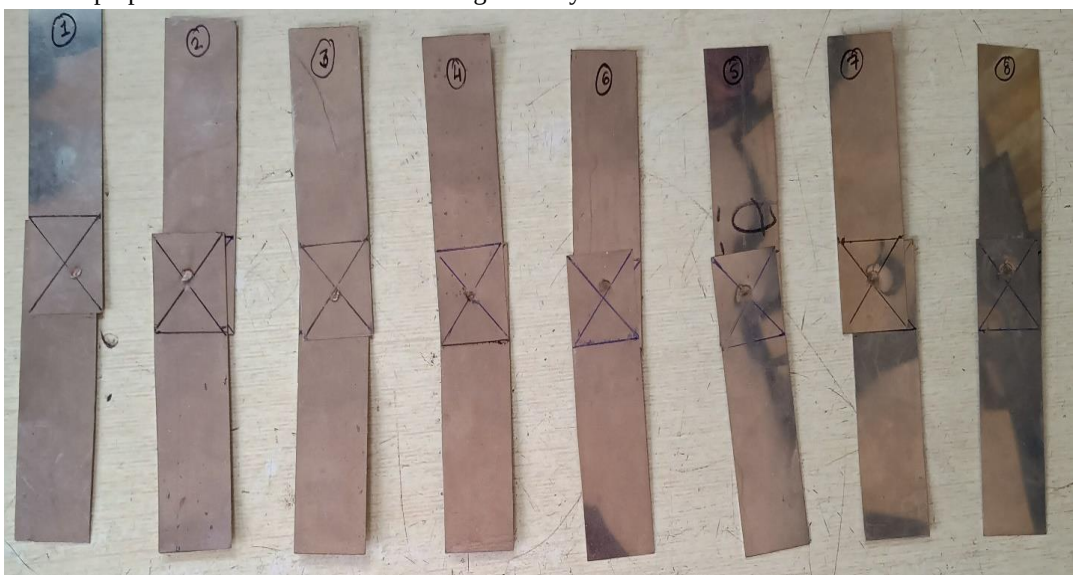

Fig. 5 Specimens prepared

3.2 Tensile testing

Destructive weld testing, as its name implies, entails the physical dismantling of a finished weld to assess its strength and properties. This testing method is commonly employed for the subsequent applications:

1. Qualification of welding procedures
2. Inspection through sampling
3. Inspection for research purposes
4. Testing the performance qualification of welders
5. Analysis of failures

Destructive weld testing methods usually entail the process of cutting or fracturing the welded component and assessing its mechanical and physical properties. For specimens with a thickness of 0.4 mm or larger, it is necessary to adjust the position of the weld grips on the test machine to minimize the eccentric loading caused by the specimen's thickness. The spot weld will experience a more accurate shear load, hence reducing the tension or peeling effect. The tension shear test is employed in production assurance testing due to its simplicity and cost-effectiveness. Coupons that have been welded at regular intervals are examined to assess the extent to which the weld schedule conforms to a pre-established standard of test results. The direct tension test is employed to quantify the tensile strength of welds when subjected to a load perpendicular to the spot interface. This test primarily serves as a means for developing weld schedules and doing research on the weldability of new materials. The direct tension test specimen is utilized to ascertain the comparative notch sensitivity of spot welds. The notch sensitivity of the weld is determined by measuring the ratio between the direct tension load and the tension shear load. For the spot weld to be termed ductile or have low-notch sensitivity, the ratio must exceed 0.5. The Universal Testing Machine (UTM) utilized for conducting tensile tests has a magnification range spanning from 0 to 40 Tons. Figure 6 shows the UTM machine used for the testing, and Figure 7 shows the clamping of the specimen on UTM.

Fig. 6 Universal Testing Machine

Fig. 7 Clamping of specimen on UTM

3.3 Microstructural analysis

Macro-etch testing refers to the process of examining the structure and properties of a material by etching a large-scale surface area. This technique necessitates the extraction of minute samples from the welded junction. Subsequently, the specimens are refined at their intersection and treated with a gentle acid blend, which varies according to the underlying substance. The acid etch technique offers a distinct and unambiguous view of the interior composition of the weld. Upon examining the etched sample, one may observe the extent to which it has penetrated. Additionally, any indications of insufficient fusion, poor penetration at the root, internal porosity, or cracking at the fusion line (the boundary between the weld and the base material) can be identified. Figure 8 is the test sample prepared and polished for moulding process.

Fig. 8 Mould of a sample after polishing and moulding process

This form of physical weld testing is employed to ascertain the integrity of a weld. The acid corrodes or interacts with the edges of fissures in the base or weld metal, thereby revealing any existing welding flaws. Additionally, it highlights the demarcation between the base material and the welded metal, so revealing the dimensions of the weld that could otherwise be unclear. Typically, this examination is conducted on a representative sample of the joint. Hydrochloric acid, nitric acid, ammonium persulfate, and iodine with potassium iodide are frequently employed for the purpose of etching carbon and low alloy steels.

4. Results and analysis

Shear test for measuring tension: The tension shear test is the predominant method employed to ascertain the strength of resistance spot welds. Additionally, it is employed for assessing the weld schedules of both ferrous and non-ferrous alloys. A universal testing machine is employed to conduct the test depicted in the picture. The

test primarily aims to determine the maximum shear strengths of the specimen when it is subjected to tension. The coupling of this test with the cross-tension test allows for the determination of the ratio between cross-tension strength and tension-shear strength, which is commonly employed as an indicator of ductility. When gaps smaller than approximately 1mm are examined, a plug is typically extracted from one sheet. This phenomenon is characteristic of a fracture resulting from the eccentric loading induced by sheets that are overlapped. As the thickness or strength of the sheet increases, the weld will break by shearing across the nugget (weld metal) at the interface. The tensile strength was determined through the execution of a tensile test using a Universal Testing Machine. To determine the size of the weld nugget, the welded samples were sliced perpendicular to their direction of welding using a basic cutting machine. By employing metallurgical polishing techniques, samples were meticulously prepared and subsequently treated with a solution for etching. The weld zone was collected in an image analyzer utilizing the interface of a metallurgical microscope, as depicted in Figure 9. Figure 9 displays a weld nugget. This encompasses its dimensions, specifically its width (W) and height (H). The dimensions of the weld nugget are determined for each sample, as indicated in Table 2.

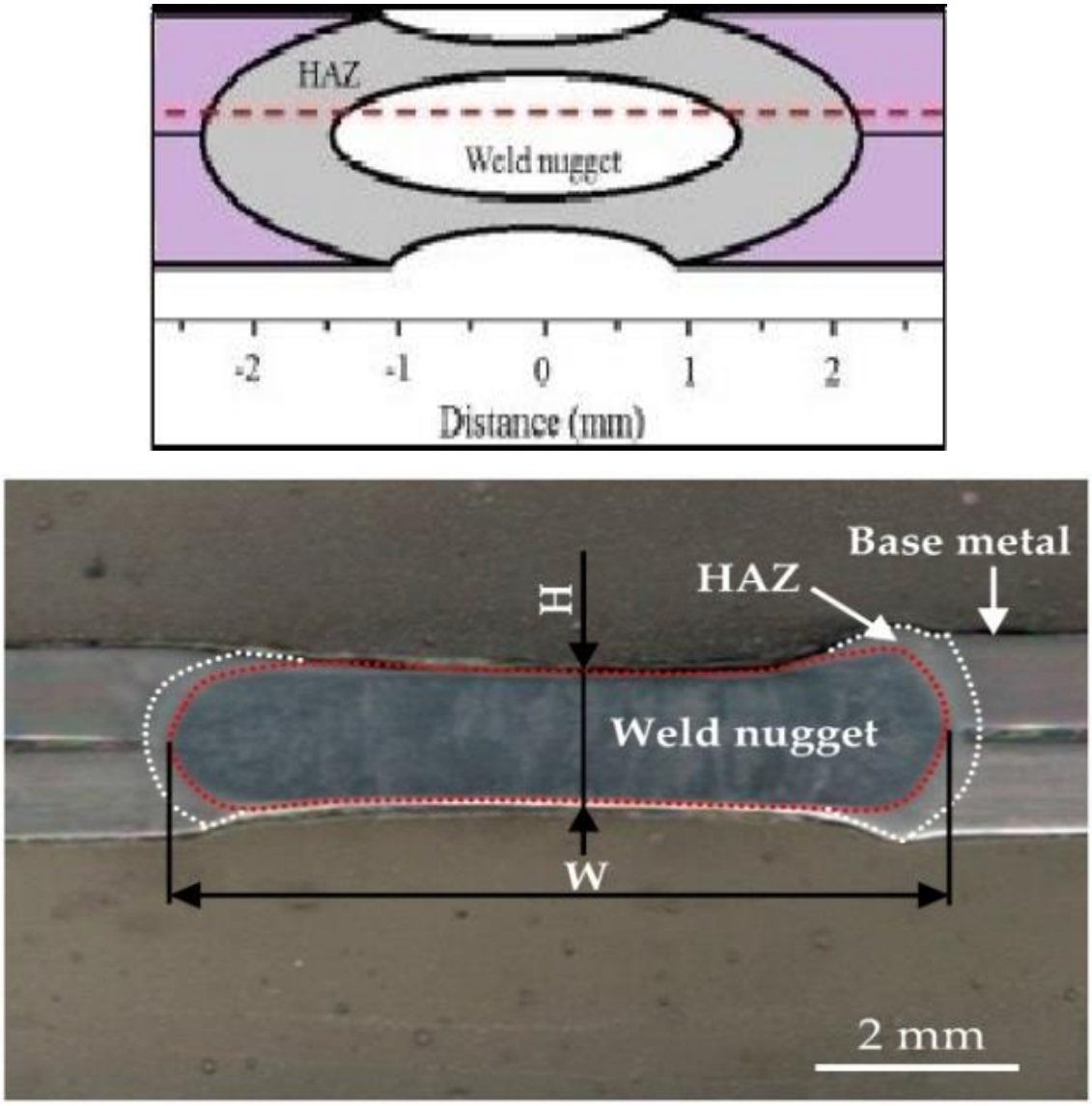

Fig. 9 Weld zone

The microstructure analysis reveals that a totally austenitic microstructure exhibits greater susceptibility to cracking compared to the microstructure that contains a minor proportion of ferrite. The microstructure of the AISI 316L stainless steel base metal consists of austenitic polygonal grains with a low proportion of delta ferrite. The grain size is classified as ASTM 7. Delta ferrite exhibits elongated stringers in the rolling direction. The microstructure of nugget is shown in the figure 10.

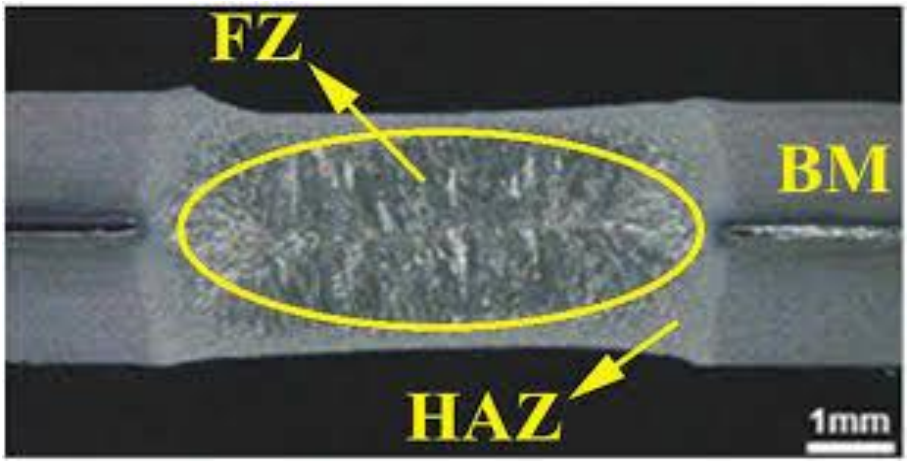

Fig. 10 Weld attributes revealed by metallographic sectioning.

The metallographic image shows the weld attributes in Figure. Three different zones are observed in the microstructure are: fusion zone (FZ), which is melted and re-solidified during the welding process and shows a cast structure with columnar grains, heat affected zone (HAZ), which is not melted but undergoes microstructural changes, and base metal (BM) which does not experience any microstructural changes.

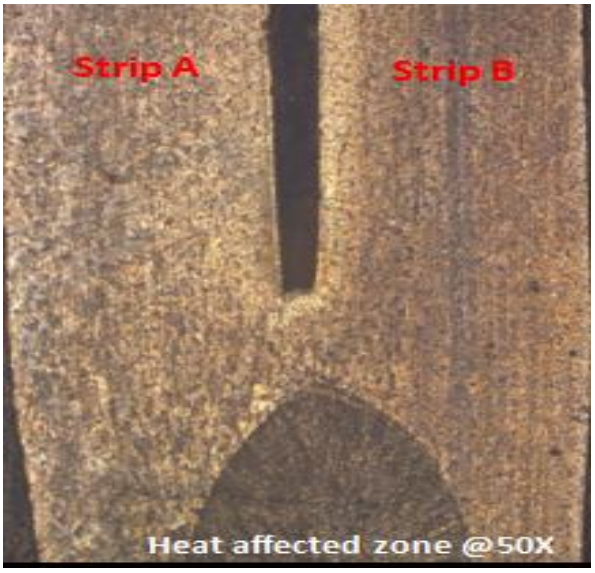

Fig. 11 Weld zone for sample 1 @ 50x

Fig. 12 Microstructure of base material

Fig. 13 Microstructure of weld zone for sample 2

Fig. 14 Microstructure of weld zone for sample 3

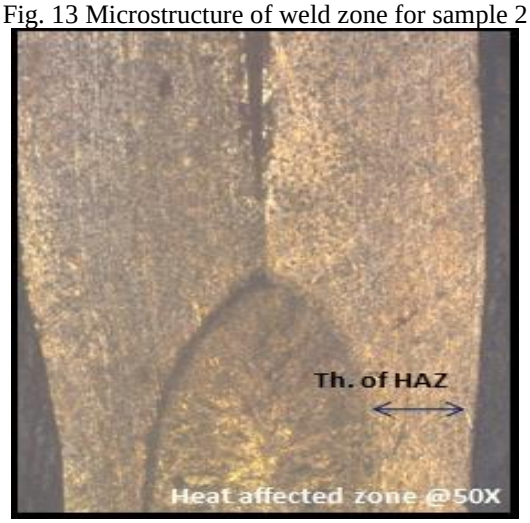

Fig. 15 Microstructure of weld zone for sample 4

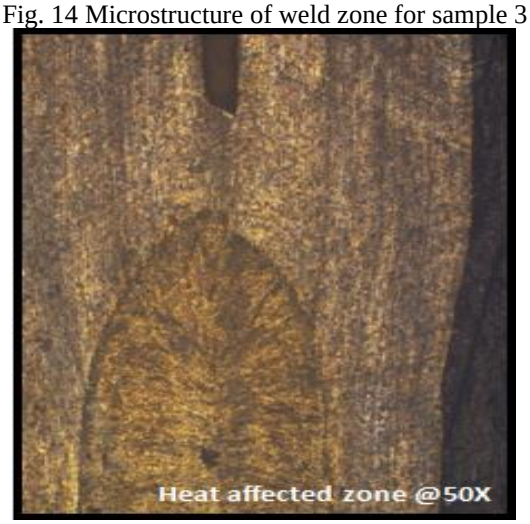

Fig. 16 Microstructure of weld zone for sample 5

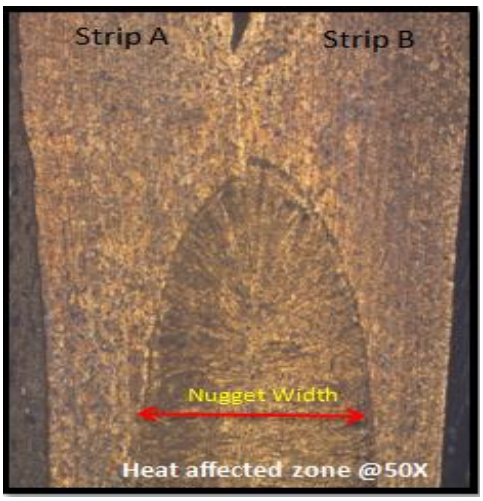

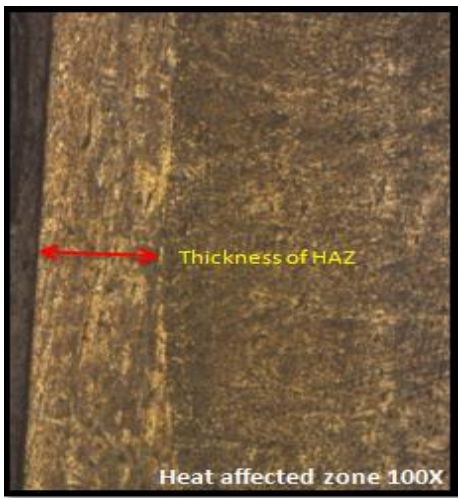

Fig. 17 and Fig. 18 Microstructure for weld zone and HAZ for sample 6 At 50X and 100 X magnification

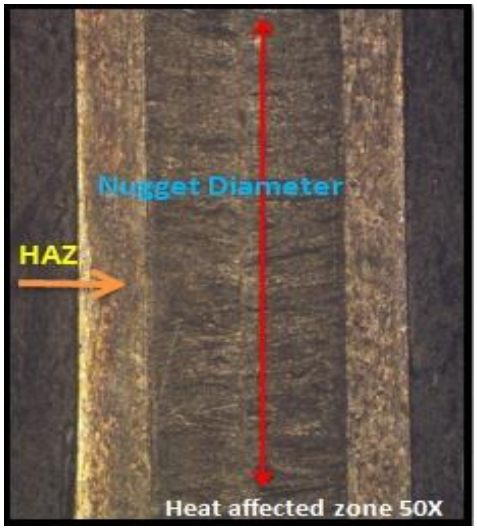

Fig. 19 and Fig. 20 Microstructure for weld zone and heat affected zone for sample 7 At 50X magnification

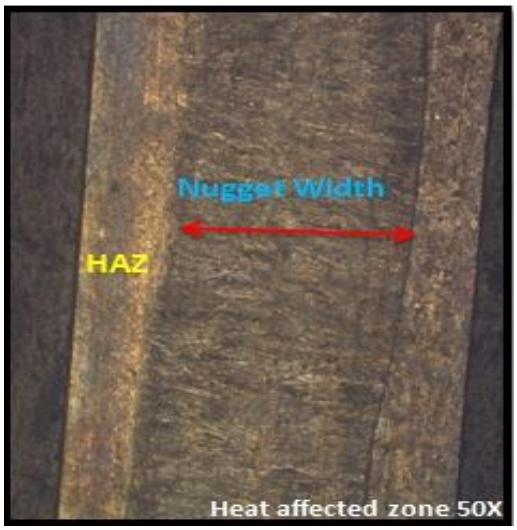

Fig. 21 and Fig. 22 Microstructure for weld zone and heat affected zone for sample 8 At 50X magnification

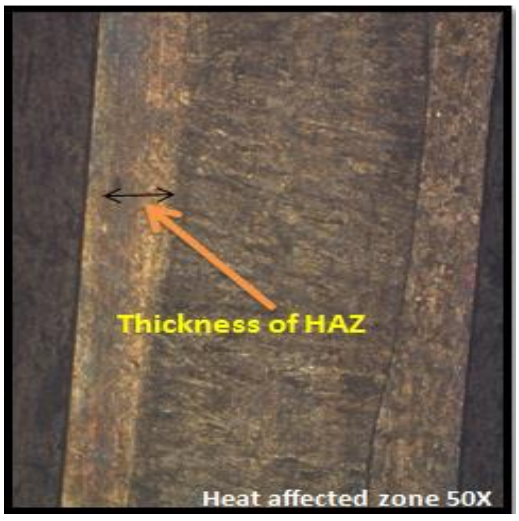

Fig. 23 and Fig. 24 Microstructure for weld zone and heat affected zone for sample 9 At 50X magnification

Fig. 25 Inverted microscope (magnification = 50x, 100x, 200x, 500x & 1000x.)

An inverted microscope is used for checking microstructure, grain size, decarburization depth, phase studies & microfine cracks. It has the 50x, 100x, 200x, 500x & 1000x magnification as shown in figure 25.

4.1 Taguchi Analysis - Analysis of Signal-to-Noise Ratio using the Taguchi Method

Parameter design investigation encompasses the examination of both control and noise variables. The signal-to-noise (S/N) ratio is used to quantify the level of interaction between various components in terms of resilience. The sensitivity of the quality characteristic under investigation was measured in a controlled manner using the signal-to-noise ratio (S/N ratio). In the context of the Taguchi method, the term 'signal' refers to the desired effect or mean value of the output characteristic. On the other hand, the term 'noise' refers to the undesired effect or signal disruption, specifically caused by external elements known as noise components, that influence the outcome. The ratio of the strength of a desired signal to the strength of background noise.

The signal-to-noise ratio (S/N ratio) is determined by equation (1) as $\eta = -10 \log (MSD)$.

The term "MSD" refers to the mean-square deviation of the output characteristic. The objective of any experiment is consistently to ascertain the utmost attainable signal-to-noise ratio for the outcome. A high signal-to-noise ratio (S/N) indicates that the signal is significantly stronger than the random disturbances caused by noise factors or minimum variance. As previously said, there are three groups of quality characteristics: those that are preferable to be lower, those that are preferable to be higher, and those that are preferable to be at a nominal level. To achieve optimal performance, it is necessary to prioritize the attribute of greater quality. The mean-square deviation (M.S.D.) for a quality feature that improves with increasing values can be calculated using the formula

$$\mathrm{MSD} = \frac{1}{n}\sum_{i=1}^{n} {y_i}^2$$

Let n be the number of repetitions or observations, and yi represent the observed data. The Taguchi approach defines the S/N ratio as the ratio between the desirable value, which is the mean of the output characteristics, and the undesirable value, which is the squared deviation of the output characteristics. The signal-to-noise ratio is a measure of the quality attributes of the observed data in the Taguchi design of the experiment. The analysis of the S/N ratio typically considers three characteristics: smaller values are preferable, higher values are preferable, and the nominal value is the most desirable. The suitable ratio is selected based on the output variable. HB incorporates measures of tensile strength and nugget diameter, both of which should ideally have higher values. Similarly, LB

encompasses the Heat Affected Zone (HAZ), where a lower value is desired. In quality engineering, features are classified as either higher the best (HB) or lower the best (LB). HB incorporates measures of tensile strength and nugget diameter, both of which should ideally have higher values. The summary statistics for the signal-to-noise ratio (S/N ratio) η (dB) are provided. The objective of this study was to achieve a high level of shear tensile strength and a well-formed weld nugget in a resistance spot-welded connection. Greater values indicate enhanced strength of the resistance spot weld joint. Consequently, a quality feature called S/N ratio, which prioritizes greater values was implemented and introduced in this study.

The formula provided relates the number of tests, denoted as 'N', to the experimental value of a certain quality feature, denoted as 'y_i', and the signal-to-noise ratio, denoted as 'η'. The value of 'η' for each experiment in L9 (OA) has been determined and recorded in the table. The table provides a summary of the signal-to-noise ratio for each level of the spot welding process parameters. Additionally, the chart also includes the calculated overall mean of the S/N ratio for the 9 trials. Table 3 is the response table for signal-to-noise (S/N) ratio maximum is the better. Table 4 is the response table for means maximum is the better.

Table 3 Response table for signal-to-noise ratios

Level	Welding current (KA) - A	Pressure (Bar) – B	Weld time (Cycles) - C
1	45.69	48.02	48.43
2	47.93	47.76	47.45
3	48.63	46.47	46.37
Delta	2.93	1.55	2.06
Rank	1	3	2

Table 4 Response table for means

Level	Welding current (KA) - A	Pressure (Bar) - B	Weld time (Cycles) - C
1	201.1	252.5	264.2
2	249.8	246.8	238.5
3	270.3	221.9	218.5
Delta	69.3	30.5	45.7
Rank	1	3	2

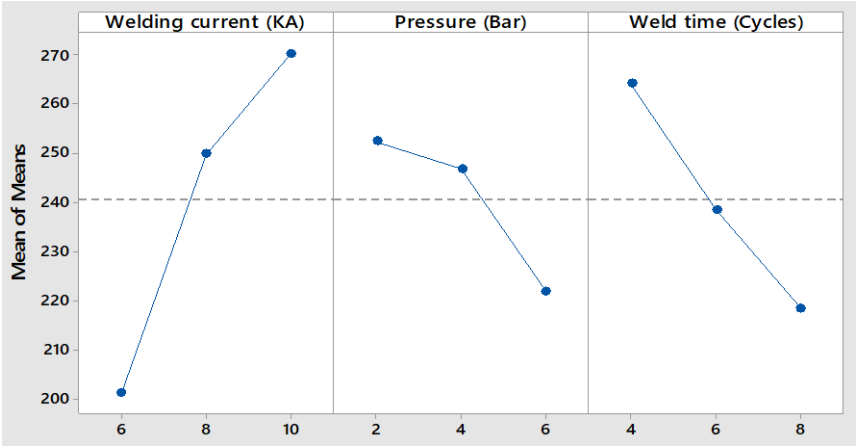

Fig. 26 Main effects plot for means

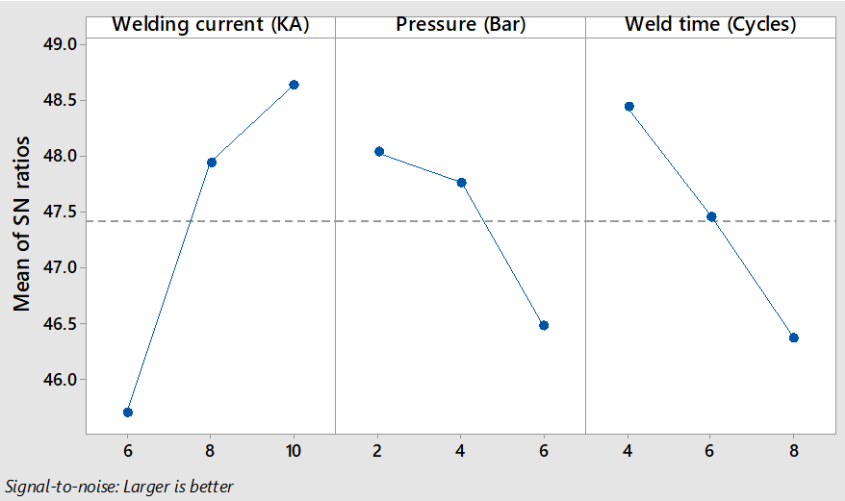

Fig. 27 Main effects plot for SN ratios

Figure 26 shows the Main effects plot for means. Figure 27 shows the S/N ratio graph where the horizontal line is the value of the total mean of the S/N ratio. Basically, the larger the S/N ratio, the better is the quality characteristic for the tensile shear strength. As per the S/N ratio analysis from the graph the levels of parameters to be set for getting optimum value of T-S strength are A3B1C1.

4.2 Effect of process parameters

4.2.1 Effect of welding current on tensile-shear strength

In low welding current application, small weld nugget diameters were obtained and similarly lower tensile-shear strength value than that of base-metal was measured due to low heat application to welding zone. However, the tensile-shear strength increases with increasing weld current. In long welding time and high welding current application, cross-section area decreases, as a result, the tensile-shear strength of the joint decreases. Electrodes react to work-piece due to excessive heating of them which cannot be compensated by cooling water. In addition, a weld nugget bursts out between two sheets resulting in a decrease in diameter.

4.2.2 Effect of welding pressure on tensile-shear strength

Increased Pressure: Higher welding pressure tends to improve the interfacial contact between the joined surfaces. This can lead to better material flow and increased bonding at the joint interface. Consequently, higher pressure often correlates with higher tensile-shear strength.

Optimal Pressure Range: There exists an optimal range of pressure for welding SS 316L sheets. Too low a pressure might result in insufficient material bonding, leading to weaker joints. Conversely, excessively high pressure might cause material deformation or expulsion, resulting in compromised joint strength.

Material Behavior: SS 316L, being a stainless steel with good ductility, can withstand moderate to high pressures without significant degradation in its mechanical properties. However, extreme pressure might induce localized stress concentrations or deformations, affecting joint integrity.

4.2.3 Effect of welding time on tensile-shear strength

Shorter Welding Time: Inadequate welding time might result in incomplete fusion or insufficient heat input, leading to weak or partial bonding at the joint interface. This can significantly reduce the tensile-shear strength of the joint.

Optimal Welding Time: There exists an optimum duration for welding SS 316L sheets, where sufficient heat input is provided to ensure proper fusion without causing excessive heat-affected zones or material degradation. This optimal time duration usually leads to stronger and more durable joints.

Prolonged Welding Time: Excessive welding time can lead to overexposure of the material to heat, causing grain growth, brittleness, or changes in microstructure, which may adversely affect the tensile-shear strength of the joint.

Interaction between Pressure and Time:

Balanced Parameters: The optimal tensile-shear strength is often achieved by a balanced combination of welding pressure and time. High pressure might compensate for shorter welding times by ensuring better material contact and increased bonding. Conversely, longer welding times might compensate for lower pressures by allowing adequate heat input for proper fusion.

Experimental Optimization: Achieving the best joint strength involves experimental optimization to find the ideal combination of welding pressure and time. This involves conducting tests with varying parameters to determine the optimal settings for SS 316L sheet joints.

5. Conclusion

In this study, the application of Taguchi method was used to obtain the optimized resistance spot welding parameters for AISI 316L steel grade sheet. ANOVA was used to determine the significance of each processing parameter. Furthermore, the predicted optimal parameters were used to determine experimental tensile strength. The following conclusions were drawn in the present study:

1. As welding time increases, the temperature of the faying surface of sheets rises quickly until this area is melted and a nugget is formed. After the formation of the nugget, the rate of temperature rise is reduced abruptly. No expulsion was observed while increasing welding time up to 8 cycles, so it seems that welding time has no significant sensitivity to expulsion.
2. Welding current is more effective on tensile strength since increasing welding time causes more heat losses from the weld zone. Welding current should be taken as much as possible while no expulsion happens to reduce the production time and improve productivity besides achieving maximum tensile strength.
3. Taguchi analysis concluded different optimum values for individual response. For maximum tensile strength, the optimum value for welding current is 10 kilo amperes, electrode pressure is 2 bar, and weld time is 4 cycles/s.
4. Percentage contribution of welding current was found to be maximum while weld time contributed moderately and pressure had the minimum contribution in the RSW process.
5. In conclusion, both welding pressure and welding time significantly impact the tensile-shear strength of SS 316L sheet joints. Optimal parameters are essential to ensure strong, durable, and reliable welded joints in this material. Balancing these parameters through experimentation and adhering to recommended guidelines can help achieve superior joint strength and overall structural integrity.

References

[1] De Castro, C. C., Shen, J., Plaine, A. H., Suhuddin, U. F., de Alcântara, N. G., dos Santos, J. F., & Klusemann, B. (2022). Tool wear mechanisms and effects on refill friction stir spot welding of AA2198-T8 sheets. Journal of Materials Research and Technology, 20, 857-866.

[2] Chaudhari, A. Y., & Deshmukh, D. D. (2020, March). Metallurgical investigations on corrosion behavior of simple and heat treated duplex stainless steel 2205 exposed to corrosive media. In IOP Conference Series: Materials Science and Engineering (Vol. 810, No. 1, p. 012048). IOP Publishing.

[3] Xiao, R., Zhao, Y., Liu, H., Oliveira, J. P., Tan, C., Xia, H., & Yang, J. (2022). Dissimilar laser spot welding of aluminum alloy to steel in keyhole mode. Journal of Laser Applications, 34(1).

[4] Baek, S., Song, J., Lee, H. C., Park, S. Y., Song, K. H., Lee, S., ... & Kim, D. (2022). Robust bonding and microstructure behavior of aluminum/high-strength steel lap joints using resistance element welding process for lightweight vehicles: Experimental and numerical investigation. Materials Science and Engineering: A, 833, 142378.

[5] Al-Ani, M. (2023, March). Investigation of mechanical and microstructural characteristics of friction stir spot welded joints of aluminum sheets. In AIP Conference Proceedings (Vol. 2651, No. 1). AIP Publishing.
[6] Reza Kashyzadeh, K., Farrahi, G. H., Minaei, M., Masajedi, R., Gholamnia, M., & Shademani, M. (2022). Numerical study of shunting effect in three-steel sheets resistance spot welding. International Journal of Engineering, 35(2), 406-416.
[7] Kalyankar, V., Bhoskar, A., Deshmukh, D., & Patil, S. (2022). On the performance of metallurgical behaviour of Stellite 6 cladding deposited on SS316L substrate with PTAW process. Canadian Metallurgical Quarterly, 61(2), 130-144.
[8] Deshmukh, D. D., & Kharche, Y. (2023). Influence of processing conditions on the tensile strength and failure pattern of resistance spot welded SS 316L sheet joint. International Journal on Interactive Design and Manufacturing (IJIDeM), 1-13.
[9] Chen, L., Zhang, Y., Xue, X., Wang, B., Yang, J., Zhang, Z., ... & Barber, G. C. (2022). Investigation on shearing strength of resistance spot-welded joints of dissimilar steel plates with varying welding current and time. Journal of Materials Research and Technology, 16, 1021-1028.
[10] Rajarajan, C., Sonar, T., Sivaraj, P., Raja, S., & Mathiazhagan, N. (2022). Investigating the effect of electrode pressure on nugget size, microstructure and tensile shear strength of resistance spot welded advanced high strength dual phase steel joints. Metallography, Microstructure, and Analysis, 11(3), 472-483.
[11] Sachin K. Dahake, Dr. Nilesh Diwakar, & Dr. Shyamkumar D. Kalpande (2023). Optimization of Resistance Spot Welding Parameters for 316L Stainless Steel Using Response Surface Methodology and Box-Behnken Design: Investigation on Joint Characteristics and Performance. Tuijin Jishu/Journal of Propulsion Technology ISSN: 1001-4055 Vol. 44 No. 5. doi: 10.52783/tjjpt.v44.i5.3003.
[12] Ghanbari, H. R., Shariati, M., Sanati, E., & Nejad, R. M. (2022). Effects of spot welded parameters on fatigue behavior of ferrite-martensite dual-phase steel and hybrid joints. Engineering Failure Analysis, 134, 106079.
[13] Betiku, O. T., Ramachandran, D. C., Ghatei-Kalashami, A., DiGiovanni, C., Sherepenko, O., Ghassemi-Armaki, H., & Biro, E. (2023). Improving the mechanical performance of press-hardened steel resistance spot welds via in-situ grain refinement. Journal of Materials Processing Technology, 320, 118122.
[14] Dong, W., Lei, M., Pan, H., Ding, K., & Gao, Y. (2022). Role of the internal oxidation layer in the liquid metal embrittlement during the resistance spot welding of the Zn-coated advanced high strength steel. Journal of Materials Research and Technology, 21, 3313-3326.
[15] Wippermann, J., Meschut, G., Koshukow, W., Liebsch, A., Gude, M., Minch, S., & Kolbe, B. (2023). Thermal influence of resistance spot welding on a nearby overmolded thermoplastic–metal joint. Welding in the World, 67(3), 793-804.
[16] Zhao, D., Vdonin, N., Radionova, L., Glebov, L., & Bykov, V. (2022). Optimization of post-weld tempering parameters for HSLA 420 steel in resistance spot welding process. The International Journal of Advanced Manufacturing Technology, 123(5-6), 1811-1823.
[17] Aswar S. J., Diwakar Nilesh & Kalpande S. D. (2023). Investigations And Optimization Of Laser Process Parameters Using Box Benhken Design Approach For Advanced Materials. Journal of Aeronautical Materials Vol. 43, Issue-01, 2023 pp. 525-542.
[18] Kakade, S., Thakur, A., Patil, S., & Deshmukh, D. (2023). Experimental evaluation and correlation of plasma transferred arc welding parameters with hardfacing defects. In Recent Advances in Material, Manufacturing, and Machine Learning (pp. 326-331). CRC Press.
[19] Guo, J., Bi, J., Wang, S., Li, Y., Manladan, S. M., & Luo, Z. (2022). Modeling the effect of electrode morphology on Mg/steel resistance spot welding. The International Journal of Advanced Manufacturing Technology, 120(1-2), 137-148.
[20] Yaghoobi, F., Jamaati, R., & Aval, H. J. (2022). Resistance spot welding of high-strength DP steel and nano/ultrafine-grained IF steel sheets. Materials Chemistry and Physics, 281, 125909.
[21] Kakade, S. P., Thakur, A. G., Deshmukh, D. D., & Patil, S. B. (2022). Experimental investigations and optimisation of Ni-Cr-B-Si hardfacing characteristics deposited by PTAW process on SS 410 using response surface method. Advances in Materials and Processing Technologies, 1-17.

[22] Chaudhari A. Y., Diwakar Nilesh & Kalpande S. D. (2023). Mechanical characteristics, morphology and corrosion behavior of duplex stainless steel 2205. Eur. Chem. Bull. 2023,12(Special issue 8), 4900-4910.

[23] Naik, H. V., Deshmukh, D. D., & Kalyankar, V. D. (2019). Study of heat treatment effect on microstructure of PTA weld deposited surface of SS 316L steel. In Advances in Additive Manufacturing and Joining: Proceedings of AIMTDR 2018 (pp. 597-607). Singapore: Springer Singapore.

[24] Kalyankar, V. D., & Deshmukh, D. D. (2017, December). Failure investigations of failed valve plug SS410 steel due to cracking. In IOP Conference Series: Materials Science and Engineering (Vol. 282, No. 1, p. 012007). IOP Publishing.

[25] Deshmukh, D. D., & Kalyankar, V. D. (2019). Deposition Characteristics of Multitrack Overlayby Plasma Transferred Arc Welding on SS316Lwith Co-Cr Based Alloy–Influence ofProcess Parameters. High Temperature Materials and Processes, 38(2019), 248-263.

[26] Deshmukh, D. D., & Kalyankar, V. D. (2018). Recent status of overlay by plasma transferred arc welding technique. International Journal of Materials and Product Technology, 56(1-2), 23-83.

[27] Deshmukh, D. D., & Kalyankar, V. D. (2019). Evaluation of surface characteristics of PTAW hardfacing based on energy and powder supplied. In Advances in Micro and Nano Manufacturing and Surface Engineering: Proceedings of AIMTDR 2018 (pp. 547-558). Singapore: Springer Singapore.

[28] Ding, K., Dong, W., Lei, M., Wang, L., Pan, H., & Gao, Y. (2022). Oxidation-assisted crack propagation of the liquid metal embrittlement in the resistance spot welded steels. Materials Characterization, 194, 112438.

[29] Manladan, S. M., Jang, Y., & Park, Y. D. (2023). Effect of paint baking on the halo ring and mechanical behavior of 30MnB5 hot-stamped steel resistance spot welding joints. Journal of Materials Research and Technology, 24, 4756-4761.

[30] Yang, Y., Li, Y., Bi, J., Liu, H., Ao, S., & Luo, Z. (2022). Microstructure and mechanical properties of 2195/5A06 dissimilar joints made by resistance spot welding. Materials Characterization, 191, 112147.

[31] Pestka, J., & Weihe, S. (2022, November). Influence of the Joining Force on the Nugget Diameter During Resistance Spot Welding of Aluminum Materials. In Stuttgart Conference on Automotive Production (pp. 96-107). Cham: Springer International Publishing.

[32] Kumar, N., Ramakrishnan, S. M., Panchapakesan, K., Subramaniam, D., Masters, I., Dowson, M., & Das, A. (2022). In-depth evaluation of micro-resistance spot welding for connecting tab to 18,650 Li-ion cells for electric vehicle battery application. The International Journal of Advanced Manufacturing Technology, 121(9-10), 6581-6597.

[33] Sharma, S. K., Patel, P., Chandra, M., Rajak, A. K., & Sharma, C. (2022). Resistance Spot Welding of Aluminum 6063 Alloy for Aerospace Application: Improvement of Microstructural and Mechanical Properties. Journal of The Institution of Engineers (India): Series D, 103(1), 311-318.

[34] Bhoskar, A., Kalyankar, V., & Deshmukh, D. (2023). Metallurgical characterisation of multi-track Stellite 6 coating on SS316L substrate. Canadian Metallurgical Quarterly, 62(4), 665-677.

[35] Hamidinejad, S., Kolahan, F., & Kokabi, A. (2012). The modelling and process analysis of resistance spot welding on galvanized steel sheets used in car body manufacturing. Materials & Design, 34, 759-767. doi: 10.1016/j.matdes.2011.06.064.